frontiers in Cell and Developmental Biology

ORIGINAL RESEARCH
published: 21 July 2021
doi: 10.3389/fcell.2021.642931

Identification of Jmjd3 as an Essential Epigenetic Regulator of *Hox* Gene Temporal Collinear Activation for Body Axial Patterning in Mice

Feng Zhang[1,2†], Xiong Zhao[3†], Runmin Jiang[4†], Yuying Wang[1], Xinli Wang[3], Yu Gu[1], Longyong Xu[5], Jing Ye[1], Charlie Degui Chen[5], Shuangping Guo[1], Dawei Zhang[3*] and Daqing Zhao[6*]*

[1] State Key Laboratory of Cancer Biology, Department of Pathology, Xijing Hospital, Fourth Military Medical University, Xi'an, China, [2] Department of Pathology, Air Force Medical Center (Air Force General Hospital), Chinese People's Liberation Army, Beijing, China, [3] Department of Orthopedics, Xijing Hospital, Fourth Military Medical University, Xi'an, China, [4] Department of Thoracic Surgery, Tangdu Hospital, The Fourth Military Medical University, Xi'an, China, [5] State Key Laboratory of Molecular Biology, Shanghai Key Laboratory of Molecular Andrology, Institute of Biochemistry and Cell Biology, Shanghai Institutes for Biological Sciences, Chinese Academy of Sciences, Shanghai, China, [6] Department of Otolaryngology, Tangdu Hospital, The Fourth Military Medical University, Xi'an, China

Body axial patterning develops *via* a rostral-to-caudal sequence and relies on the temporal colinear activation of *Hox* genes. However, the underlying mechanism of *Hox* gene temporal colinear activation remains largely elusive. Here, with small-molecule inhibitors and conditional gene knockout mice, we identified Jmjd3, a subunit of TrxG, as an essential regulator of temporal colinear activation of *Hox* genes with its H3K27me3 demethylase activity. We demonstrated that Jmjd3 not only initiates but also maintains the temporal collinear expression of *Hox* genes. However, we detected no antagonistic roles between Jmjd3 and Ezh2, a core subunit of PcG repressive complex 2, during the processes of axial skeletal patterning. Our findings provide new insights into the regulation of *Hox* gene temporal collinear activation for body axial patterning in mice.

Keywords: Jmjd3, Ezh2, H3K27me3, homeotic transformation, temporal collinearity of *Hox* gene activation, chondrogenic cells

OPEN ACCESS

Edited by:
Claire Rougeulle, UMR7216 Epigénétique et Destin Cellulaire, France

Reviewed by:
Toshiro Iwagawa, The University of Tokyo, Japan
Valentina Massa, University of Milan, Italy

***Correspondence:**
Feng Zhang
zhf1975@fmmu.edu.cn
Dawei Zhang
zdwyxj@163.com
Daqing Zhao
zhaodq430@163.com

† These authors have contributed equally to this work

Specialty section:
This article was submitted to Developmental Epigenetics, a section of the journal Frontiers in Cell and Developmental Biology

Received: *17 December 2020*
Accepted: *23 June 2021*
Published: *21 July 2021*

Citation:
Zhang F, Zhao X, Jiang R, Wang Y, Wang X, Gu Y, Xu L, Ye J, Chen CD, Guo S, Zhang D and Zhao D (2021) Identification of Jmjd3 as an Essential Epigenetic Regulator of Hox Gene Temporal Collinear Activation for Body Axial Patterning in Mice. Front. Cell Dev. Biol. 9:642931. doi: 10.3389/fcell.2021.642931

INTRODUCTION

The development of the mammalian body axis is a continuous process *via* a rostral-to-caudal sequence (Deschamps and Duboule, 2017; Mongera et al., 2019). The morphological characteristics of each part of the body axis are mainly determined by a "Hox code" (Kessel and Gruss, 1991; Alexander et al., 2009; Wellik, 2009). *Hox* genes were first discovered in *Drosophila* (Lewis, 1978). Mammals have 39 Hox genes, which are divided into four clusters. Each cluster locates on different chromosomes and has 9–11 *Hox* genes. According to the sequence homologies and their position within the cluster, the *Hox* genes are divided into 1–13 paralog groups (PGs) (Casaca et al., 2014). The function of *Hox* genes in the same PG is similar and can be mutually replaced (Wellik, 2009).

The expression of *Hox* genes in mammals is characterized by spatial collinearity, which means that the sequence of the *Hox* gene cluster from 3′ to 5′ on chromosomes corresponds to the expression domain of *Hox* genes *via* a rostral-to-caudal sequence on the body axis (Deschamps and van Nes, 2005; Montavon and Soshnikova, 2014; Deschamps and Duboule, 2017). Thus, the inactivation of 3′ *Hox* genes leads to the altered identities in the rostral side of the body axis, while the loss of 5′ *Hox* genes causes the morphological change of caudal segments (Deschamps and van Nes, 2005; Montavon and Soshnikova, 2014; Deschamps and Duboule, 2017). Interestingly, establishment of spatial collinear *Hox* gene expression relies on the temporal collinear activation of *Hox* genes in mice (Deschamps and van Nes, 2005; Montavon and Soshnikova, 2014; Deschamps and Duboule, 2017). In other words, *Hox* genes become activated in a time order corresponding to their location within the clusters (Montavon and Soshnikova, 2014; Deschamps and Duboule, 2017; Krumlauf, 2018). At E7.2, the 3′ *Hox* genes are firstly expressed in the posterior primitive streak, and over time, the expression of *Hox* genes gradually transited to the more 5′ *Hox13* PGs at E9.5 (Deschamps and van Nes, 2005; Soshnikova and Duboule, 2009; Montavon and Soshnikova, 2014; Deschamps and Duboule, 2017). Synchronization with the initiation order of *Hox* gene activation and *Hox* gene expression domains start to spread rostrally from the primitive streak, then the expression of 3′ *Hox* genes spreads to the more rostral side, while the 5′ *Hox* genes were expressed in the more caudal segments (Deschamps and van Nes, 2005; Montavon and Soshnikova, 2014; Deschamps and Duboule, 2017). Temporal collinear abnormalities of *Hox* genes will lead to corresponding morphological alterations of the *Hox* gene that spatially expresses the domain *via* a rostral-to-caudal sequence on the body axis. For example, deletion of the *Hoxc8* enhancer causes a transient delay in the initial transcription of the *Hoxc8* gene and results in homeotic transformations, which phenocopies the axial defects of the *Hoxc8*-null mutant in mice (Juan and Ruddle, 2003). On the contrary, a precocious expression of *Hox13* genes causes premature arrest of posterior axial growth (Young et al., 2009). Therefore, the accurately spatiotemporal expression of *Hox* genes is essential for correct body axis patterning.

The initiation of body axis patterning is proposed by signal molecules. For example, embryos *of Wnt3* inactivation do not express any *Hox* genes (Liu et al., 1999). Pre-gastrulation embryos exposed to the Wnt agonist precociously express *Hoxa1* and *Hoxb1* (Neijts et al., 2016). Homozygous *Wnt-3a* mutant mice exhibit homeotic transformations in the vertebrae along their entire body axis (Ikeya and Takada, 2001). These results suggest that Wnt3 is required for the *Hox* gene activation and body axis patterning. After initiation of expression, the transcriptional pattern of *Hox* genes is maintained by the antagonistic complex Polycomb (PcG) and Trithorax (TrxG) (Geisler and Paro, 2015; Piunti and Shilatifard, 2016). PcG generally maintain *Hox* gene repression, while TrxG counteract PcG and maintain the active expression state of *Hox* genes (Mallo and Alonso, 2013; Montavon and Soshnikova, 2014). PcG genes were originally identified in *Drosophila*. Mutations in PcG genes cause ectopic *Hox* gene expression, resulting in posterior homeotic transformations (Simon et al., 1992; Montavon and Soshnikova, 2014). TrxG genes were discovered to suppress the homeotic phenotypes displayed by PcG mutants (Kennison and Tamkun, 1988). Biochemical studies have revealed that PcG and TrxG form multiprotein complexes containing both histone methyltransferase and demethylases activities, respectively. For example, Ezh2 (Kmt6b) is a core subunit of PcG repressive complex 2 (PRC2) and inhibits *Hox* gene transcription by establishment of repressed histone modification H3K27 trimethylation (H3K27me3) with its histone methyltransferase activity (Cao et al., 2002; Czermin et al., 2002; Kuzmichev et al., 2002; Muller et al., 2002). H3K27me3 can be removed by histone demethylases Utx (Kdm6a) and Jmjd3 (Kdm6b) (Agger et al., 2007; De Santa et al., 2007; Hong et al., 2007; Lan et al., 2007), which belong to the TrxG group for the biochemical association with Mll2 or RbBP5 (De Santa et al., 2007; Lee et al., 2007). Interestingly, a ChIP-seq study found that the temporal collinear activation of *Hox* genes was accompanied with a sequential elimination of repressive marker H3K27me3 on the *Hox* genes (Soshnikova and Duboule, 2009; Noordermeer et al., 2014). Using high-resolution chromatin conformation capture methodology, Noordermeer et al. detected newly activated *Hox* genes progressively clustering into a transcriptionally active compartment from a transcriptionally inactive *Hox* gene cluster after transcription starts; thus, the *Hox* gene clusters switch to a bimodal 3D organization. This transition in spatial configurations coincides with the dynamical erase of H3K27me3 on the *Hox* gene clusters (Noordermeer et al., 2011, 2014). However, to date a rare epigenetic regulator for temporal collinear activation of *Hox* genes has been identified. Moreover, whether PcG and TrxG complexes antagonistically adjust the temporary collinear activation of *Hox* genes is not strictly examined in mammals.

Due to obvious morphological differences of each part, axial skeleton is an ideal model to study the relation between *Hox* gene expression and morphogenesis of the body axis (Wellik, 2009). Here, with the axial bone as a model, combined with conditional genetic deletion and biochemical techniques, we identified Jmjd3 as an essential epigenetic regulator of *Hox* gene temporal colinear activation for mouse body axial patterning. Furthermore, we detected no dynamical interplay between Jmjd3 and Ezh2 during the process of axial skeletal patterning in mice.

RESULTS

Jmjd3 Is a Potential Candidate Epigenetic Regulator of *Hox* Gene Temporal Collinear Activation

The temporal collinear activation of mouse *Hox* genes occurs at the embryonic stage of E7.2–E9.5 days (Deschamps and van Nes, 2005; Soshnikova and Duboule, 2009; Deschamps and Duboule, 2017). To identify the epigenetic regulators of *Hox* gene temporal collinear activation, we profiled the expression of 17 histone methyltransferases and 28 histone demethylases in E7.5, E8.5, and E9.5 embryonic

tissues. Among these tissues, E7.5 tissue was from the whole mouse embryos, while E8.5 and E9.5 tissues were from the trunk of embryos, as previously described (Soshnikova and Duboule, 2009). Compared with E7.5 embryos, real-time reverse transcriptase-quantitative polymerase chain reaction (RT-qPCR) revealed that, except for a few silenced genes, most histone methyltransferases were significantly activated in E9.5 embryos instead of either E7.5 or E8.5 embryonic tissues (**Supplementary Figure 1A**). Because most *Hox* genes had been activated at E9.5 days (Deschamps and van Nes, 2005; Soshnikova and Duboule, 2009; Deschamps and Duboule, 2017), these results indicated that most histone methyltransferases might not be essential for the temporal collinear activation of *Hox* genes. Interestingly, although half of the 28 histone demethylases genes were silenced, *Kdm6b* (*Jmjd3)* was significantly successively activated during the E7.5–E9.5 stages (**Supplementary Figure 1B**). Jmjd3 is a potent H3K27me3 demethylase (Agger et al., 2007; De Santa et al., 2007; Lan et al., 2007). A previous report showed that the temporal collinear activation of *Hox* genes was accompanied with the progressive elimination of H3K27me3 on *Hox* genes (Soshnikova and Duboule, 2009). Therefore, these results suggest that Jmjd3 is a potential candidate for the regulation of *Hox* gene temporal collinear activation.

Jmjd3 Rather Than Utx Is Required for Mouse Body Axis Patterning

Both Jmjd3 and Utx are potent H3K27me3 demethylases. Previously, Utx was demonstrated to be required for the body axis patterning of zebrafish and *Drosophila* (Lan et al., 2007; Copur and Muller, 2013, 2018). To test the roles of Utx and Jmjd3 during body axis patterning in mice, we conditionally delete *Utx* or *Jmjd3* in uncommitted mesenchymal cells of mice, respectively. Skeleton assays revealed, in addition to the fusions of C1 and C2 and sternal asymmetries, that no obvious homeotic transformations in the vertebrae along the entire body axis in $Utx^{fl/Y}$;*Prx1-Cre* (0/25) or $Utx^{fl/fl}$;*Prx1-Cre* (0/22) mice (**Supplementary Figure 2** and **Table 1**) was detected. This indicated Utx is not required for mouse axial skeletal patterning. However, the phenotypes of $Jmjd3^{fl/fl}$;*Prx1-Cre* mice were very similar to those of $Jmjd3^{fl/fl}$;*EIIa-Cre* mice as previously described for E18.5 (Zhang et al., 2015). Both embryos have dwarfism with thoracic kyphosis (**Supplementary Figure 2**; Zhang et al., 2015). The complete fusions of C1 and C2 (14/14) were detected in $Jmjd3^{fl/fl}$;*Prx1-Cre* mice. Homeotic transformations in the vertebrae along the whole-body axis in $Jmjd3^{fl/fl}$;*Prx1-Cre* mice were visibly detected, including anterior transformation of C2 to C1 (an extra ventral tubercle shared by fused C1 and C2, 14/14), T1 to C7 (T1 without ribs or with incomplete ribs, 7/14), T3

TABLE 1 | [a]Homeotic transformations of axial skeletons with various genotypes.

Genotypes	Time points	Total (*n*)	Homeotic transformations of axial skeletons						
			[b]C2 to C1	[c]T1 to C7	[d]T3 to T2	[e]T8 to T7	[f]L1 to T13	[g]S1 to L6	[h]L6 to S1
[i]Control		60							4 (6.7%)
$Jmjd3^{fl/+}$;*Prx1-Cre*		10	1 (10.0%)				7 (70.0%)		
$Jmjd3^{fl/fl}$;*Prx1-Cre*		14	14 (100%)	7 (50.0%)	3 (21.4%)		14 (100%)	10 (100%)	
$Utx^{fl/Y}$;*Prx1-Cre*		25							1 (4.0%)
$Utx^{fl/fl}$;*Prx1-Cre*		22							2 (9.0%)
$Ezh2^{fl/+}$;*Prx1-Cre*		17							10 (58.8%)
$Ezh2^{fl/fl}$;*Prx1-Cre*		15							7 (46.7%)
$Jmjd3^{fl/fl}$;*Col2a1-Cre*^{ERT2}	E8.5	18	7 (38.9%)	10 (55.6%)	6 (33.3%)	16 (88.9%)	18 (100%)	9 (50%)	
	E9.5	17				15 (88.2%)	17 (94.4%)	13 (76.5%)	
	E10.5	21				3 (14.2%)	4 (19.0%)		
$Ezh2^{fl/fl}$;*Col2a1-Cre*^{ERT2}	E8.5	20							12 (60.0%)
	E9.5	21							10 (47.6%)
	E10.5	16							7 (43.8%)
$Jmjd3^{fl/fl}$;$Ezh2^{fl/fl}$;*Col2a1-Cre*^{ERT2}	E8.5	12	5 (41.7%)	8 (66.7%)	5 (41.7%)	10 (83.3%)	12 (100%)	9 (75.0%)	
	E9.5	10				8 (80.0%)	9 (90.0%)	5 (50.0%)	
	E10.5	25				4 (16.0%)	5 (20.0%)	3 (12.0%)	

[a]*Numbers of mice in each category are shown. Both unilateral and bilateral abnormalities were included in axial skeleton analysis. Number of sacral vertebrae was not counted because the cartilaginous linkages between the sacral vertebrae S3 and S4 are often only very fine at birth.*
[b]*An extra ventral tubercle shared by fused C1 and C2.*
[c]*T1 without ribs or with incomplete ribs.*
[d]*Longest spinous process on T3 instead of T2.*
[e]*T8 with unilateral or bilateral vertebrosternal ribs.*
[f]*L1 with a pairs of complete or incomplete ribs.*
[g]*S1 without bilateral or unilateral iliac bones.*
[h]*L6 with bilateral or unilateral iliac bones.*
[i]*Mice of control group including the genotypes of Col2a1-Cre^{ERT2}, $Jmjd3^{fl/fl}$, $Utx^{fl/fl}$, and $Ezh2^{fl/fl}$, each genotype contain 15 mice.*
C, cervical; T, thoracic; L, lumbar; S, sacral; WT, wild type.

to T2 (longest spinous process on T3 instead of T2,3/14), L1 to T13 (L1 with a pairs of complete or incomplete ribs, 14/14), and S1 to T6 (S1 without bilateral or unilateral iliac bones, 10/14) (**Supplementary Figure 2** and **Table 1**). In addition, some anterior transformations, such as L1 to T13 (7/10), were also detected in *Jmjd3*$^{fl/+}$;*Prx1*-Cre embryos, indicating the dose effect of Jmjd3 on axial skeletal patterning (**Supplementary Figure 2** and **Table 1**). Consistently, RNA-seq assays indicated that Jmjd3 loss in uncommitted mesenchymal cells mildly decreased the expression of *Hox3–5* PGs but markedly reduced the mRNA level of *Hox6–10* PGs compared to WT in E8.5 littermates (**Supplementary Figures 3**, **4** and **Supplementary Table 2**). Therefore, these results indicated that Jmjd3 rather than Utx is required for mouse body axis patterning.

Jmjd3 Temporally Regulates the Axial Skeletal Patterning of Mice With Its H3K27me3 Demethylase Activity

Jmjd3 deletion in uncommitted mesenchymal cells leads to the homeotic transformation in the vertebrae along the whole-body axis (**Supplementary Figure 2** and **Table 1**). To test whether Jmjd3 temporally regulates the axial skeletal patterning with its H3K27me3 demethylase activity, we tested the role of GSK-J4, an inhibitor of Jmjd3 (Ntziachristos et al., 2014), on body axis patterning *in vivo*. One dose of GSK-J4 (50 mg/kg) treatment at E8.5 induced only anterior transformation of T8 to T7 (26/26) at the middle part of the trunk but not at the cervical, lumbar, and sacral segments of E18.5 mice (**Figures 1A,B** and **Table 2**). GSK-J4 treatment at E9.5 produced homeotic transformations of L1 to T13 (15/15) and S1 to T6 (14/15) in the caudal half of the vertebral column of E18.5 mice (**Figures 1A,B** and **Table 2**). GSK-J4 treatment at E10.5 produced no obvious homeotic transformations in E18.5 mouse embryos (**Figures 1A,B** and **Table 2**). These were consistent with previous reports that *Hox* genes of the middle part or 5′ end of the *Hox* gene cluster were activated at E8.5 or E9.5, respectively (Deschamps et al., 1999; Kmita and Duboule, 2003; Deschamps and van Nes, 2005; Soshnikova and Duboule, 2009). GSK-J4 treatment at E8.5 or E9.5 induced anterior transformation at the corresponding part of axial skeletal patterning, strongly supporting that Jmjd3 temporally regulates the axial patterning of mice with its H3K27me3 demethylase activity.

Jmjd3 Regulated *Hox* Gene Temporal Collinear Activation With Its H3K27me3 Demethylase Activity

In murine embryos, *Hox* genes at the 3′ end of *Hox* clusters are first activated at E7.2 (Deschamps and Wijgerde, 1993; Forlani et al., 2003) and the last *Hox* genes at the 5′ end of *Hox* clusters complete the transcription at around E9.5 (Deschamps et al., 1999; Kmita and Duboule, 2003; Deschamps and van Nes, 2005; Soshnikova and Duboule, 2009). Subsequently, the transcriptional states of *Hox* genes at each segment are memorized along the rostral-to-caudal axis and ultimately determine body axial patterning (Kmita and Duboule, 2003; Deschamps and van Nes, 2005). A previous investigation indicated that the temporal collinear activation of *Hox* genes was accompanied with a sequential elimination of H3K27me3 on the *Hox* genes during the process of body axis patterning (Soshnikova and Duboule, 2009; Noordermeer et al., 2014). To test whether Jmjd3 regulates the *Hox* gene temporal collinear activation with its H3K27me3 demethylase activity, we firstly examined the mRNA level of *Hox* genes after GSK-J4 treatment at different time points. Consistent with the anterior transformation of T8 to T7 in the middle part instead of the cervical, lumbar, and sacral segments of mouse embryos induced by GSK-J4 at E8.5 (**Figures 1A,B** and **Table 2**), GSK-J4 treatment at E8.0 significantly reduced the mRNA level of *Hox*8–9 PGs, which are responsible for the establishment of the T7 and T8 patterns (Favier and Dolle, 1997; Wellik, 2009), but did not affect the mRNA levels of other *Hox* PGs, such as *Hox*1–6 PGs in E8.5 mouse embryos (**Figure 2A** and **Supplementary Figure 5A**). Correspondingly, GSK-J4 treatment at E9.0 significantly reduced the mRNA level of *Hox11–13* PGs (**Supplementary Figures 5A**, **6A**) in E9.5 mouse embryos, which was consistent with the GSK-J4 treatment at E9.5 which produced anterior transformations of the vertebrae only at the caudal part of the vertebral column, including L1 to T13 and S1 to T6 (**Figures 1A,B** and **Table 2**). To investigate the reason for the mRNA level reduction on *Hox*8–9 PGs in E8.5 embryos or on *Hox11–13* PGs in E9.5 embryos by GSK-J4 treatment, we examined the H3K27me3 and Jmjd3 levels on the *Hox* genes by ChIP-qPCR assays. GSK-J4 treatment at E8.0 or E9.0 significantly increased the level of H3K27me3 on the gene body of *Hox*8–9 PGs in E8.5 embryos (**Figure 2B** and **Supplementary Figures 5A**, **13**) or *Hox*10–13 PGs in E9.5 embryos, respectively (**Supplementary Figures 5A**, **6B**, **13**). Therefore, the mRNA level reduction on *Hox*8–9 PGs in E8.5 embryos or on *Hox11–13* PGs in E9.5 embryos by GSK-J4 treatment was associated with the increased level of H3K27me3 on corresponding *Hox* genes. That is, Jmjd3 regulated *Hox* gene temporal collinear activation with its H3K27me3 demethylase activity. In addition, at E8.5 embryos, the signal of Jmjd3 was detected on *Hox*1–9 PGs but not *Hox*10–13 PGs by ChIP-qPCR assays (**Figure 2C** and **Supplementary Figure 13**). At E9.5, the signal of Jmjd3 was detected on the whole *Hox*1–13 PGs (**Supplementary Figures 6C**, **13**). These results indicated that Jmjd3 bound to *Hox* genes with a temporal collinear manner and was consistent with *Hox* gene temporal collinear activation.

Jmjd3 Temporally Regulated Axial Skeletal Patterning in Chondrogenic Cells

Axial skeletal formation starts from the differentiation of condensed mesenchymal cells to cartilaginous templates (Karsenty, 2008; Long and Ornitz, 2013). To test whether chondrogenic cells are essential for Jmjd3-mediating axial skeletal patterning in mice, *Jmjd3*$^{fl/fl}$;*Col2a1-Cre*^{ERT2} mice were generated by crossing mice with *Jmjd3*$^{fl/fl}$ and *Col2a1-Cre*^{ERT2} genotypes. The expressing Cre recombinase in chondrogenic cells of *Col2a1-Cre*^{ERT2} mice can be activated by tamoxifen. *Jmjd3*$^{fl/fl}$;*Col2a1-Cre*^{ERT2} pregnant mice were intraperitoneally injected by tamoxifen in a single dose (50 mg/kg) at a time point

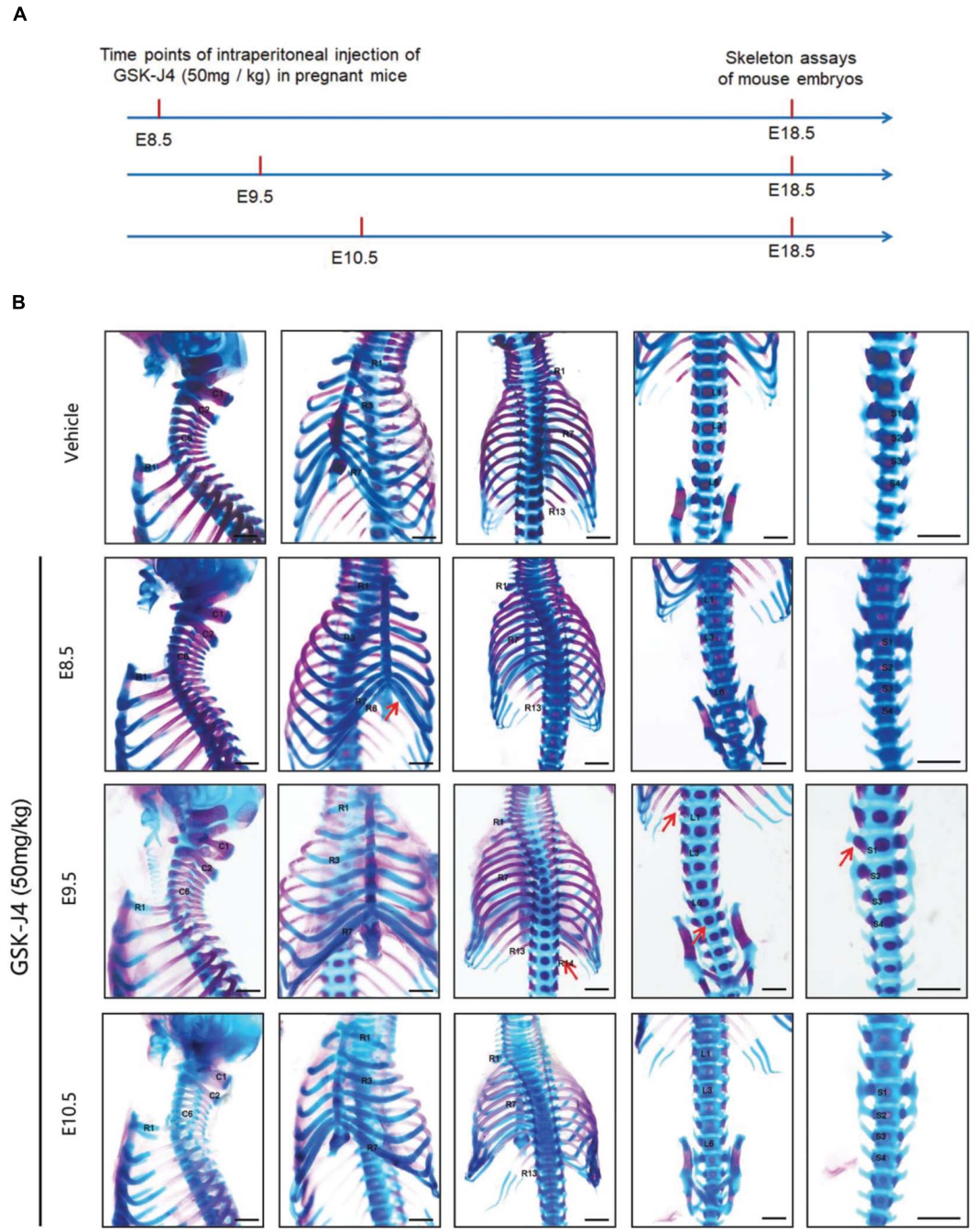

FIGURE 1 | Homeotic transformations by GSK-J4 treatment at the time points of E8.5, E9.5, or E10.5. **(A)** Experimental design for studying the roles of GSK-J4 on body axis patterning. **(B)** Embryos had been exposed to GSK-J4 at the time points of E8.5, E9.5, or E10.5 as indicated. Skeletal phenotypes were prepared by removing forelimbs and hindlimbs. The red arrow indicates homeotic transformations of axial skeleton induced by GSK-J4. Frequencies of homeotic transformations are given in **Table 1**. The cervical (C), rib (R), lumbar (L), and sacral (S) vertebrae are numbered. For schematic explanation, see **Supplementary Figure 9**. Scale bar, 1 mm.

from E8.5 to E10.5. Interestingly, different from the phenotypes of GSK-J4 treatment at E8.5, *Jmjd3* knockout in chondrogenic cells at E8.5 induced more broadness and frequency of axial skeletal abnormalities along the whole-body axis of E18.5 embryos, primarily exhibiting anterior transformation of C2 to C1 (7/18), T1 to C7 (10/18), T3 to T2 (6/18), T8 to T7 (16/18), L1 to T13 (18/18), and S1 to T6 (9/18) (**Figures 3A,B** and **Tables 1**, **2**). Similarly, different from the phenotypes induced by GSK-J4 treatment at E9.5, *Jmjd3* knockout by tamoxifen at E9.5 induced homeotic transformations of T8 to T7 (15/17), L1 to T13

TABLE 2 | Skeletal analysis of E18.5 mouse embryos after treatment by GSK-J4 (50 mg/kg) or GSK-126 (100 mg/kg) at the indicated time points[a].

Inhibitors	Vehicle	GSK-J4			GSK-126		
Time points		**E8.5**	**E9.5**	**E10.5**	**E8.5**	**E9.5**	**E10.5**
Total number of mice	**46**	**26**	**15**	**25**	**29**	**17**	**16**
Homeotic transformation of axial skeletons							
[b]T8 to T7		26 (100%)					
[c]L1 to T13			15 (100%)				
[d]S1 to L6			14 (93.3%)				
[e]L6 to S1	2 (4.3%)	1 (3.8%)	0 (0%)	1 (4%)	9 (31.0%)	5 (29.4%)	4 (25.0%)

[a]*Numbers of mice in each category are shown, and all mice were of hybrid background. Both unilateral and bilateral abnormalities were included in axial skeleton analysis. Number of sacral vertebrae was not counted because the cartilaginous linkages between the sacral vertebrae S3 and S4 are often only very fine at birth.*
[b]*T8 with unilateral or bilateral vertebrosternal ribs.*
[c]*L1 with a pairs of complete or incomplete ribs.*
[d]*S1 without bilateral or unilateral ilial bones.*
[e]*L6 with bilateral or unilateral ilial bones.*
C, cervical; T, thoracic; L, lumbar; S, sacral.

(17/17), and S1 to T6 (13/17) at the thoracic, lumbar, and sacral regions of E18.5 mouse embryos (**Figures 3A,B** and **Tables 1**, **2**). Lastly, although GSK-J4 treatment at E10.5 induced no visible homeotic transformations along the axial skeleton (**Figures 1A,B** and **Table 2**), *Jmjd3* conditional deletion by tamoxifen at E10.5 produced, though with less frequency, homeotic transformations of T8 to T7 (3/21) and L1 to T13 (4/21) at the thoracic and lumbar segments of E18.5 embryos (**Figures 3A,B** and **Table 1**). These results indicate that *Jmjd3* knockout in chondrogenic cells produces more broadness and frequency of homeotic transformations along the whole-body axis than those induced by GSK-J4 at the same time points.

Jmjd3 Temporally Activated and Maintained *Hox* Gene Expression in Mice

Different from the effects of GSK-J4 treatment, conditional deletion of *Jmjd3* at the same time points in chondrogenic cells produced more broadness and frequency of anterior transformation of axial skeleton (**Figures 1A,B**, **3A,B** and **Tables 1**, **2**). Previous results showed that, additionally as an H3K27m3 demethylase, Jmjd3 maintains a gene expression independent of H3K27m3 demethylase activity in differentiated cells (Miller et al., 2010) or during the process of early embryonic development (Shpargel et al., 2014). Therefore, we speculated that Jmjd3 in chondrogenic cells might not only mediate the *Hox* gene temporal colinear activation but also maintain *Hox* gene expression after their transcription activation. To test the hypothesis, we examined the effect of *Jmjd3* deletion on the mRNA level of *Hox* PGs during body axis patterning. Interestingly, *Jmjd3* knockout by tamoxifen at E8.0 reduced the mRNA level of *Hox3–9* PGs in E8.5 embryos (**Figure 4A** and **Supplementary Figure 5B**). However, GSK-J4 treatment at E8.0 only decreased the mRNA level of *Hox8–9* PGs in E8.5 embryos (**Figure 2A** and **Supplementary Figure 5A**). Knockout of *Jmjd3* at E9.0 by tamoxifen significantly decreased the expression level of *Hox8–13* PGs (**Supplementary Figures 5B**, **7A**) in E9.5 embryos, while GSK-J4 treatment at E9.0 only reduced the transcriptional level of *Hox11–13* PGs in E9.5 embryos (**Supplementary Figures 5A**, **6A**). *Jmjd3* deletion in chondrogenic cells obviously affected more *Hox* PG expression than those by GSK-J4 treatment at the same time points. These results were consistent with the fact that *Jmjd3* deletion by tamoxifen produced more broadness and frequency of anterior transformation of axial skeleton than those by GSK-J4 treatment at the same time points (**Figures 1A,B**, **3A,B**). Consistently, tamoxifen instead of GSK-J4 treatment at E8.0 significantly reduced the level of Jmjd3 protein on the *Hox3–9* PGs in E8.5 embryos (**Figures 2C**, **4C** and **Supplementary Figures 5A,B**, **13**). However, *Jmjd3* deletion only increased the H3K27me3 level on *Hox8–9* PGs instead of *Hox3–7* PGs (**Figure 4B** and **Supplementary Figures 5B**, **13**). Because GSK-J4 treatment also only increased the H3K27me3 level on *Hox8–9* PGs but not on *Hox3–7* PGs (**Figure 2B** and **Supplementary Figures 5A**, **13**), these results support that Jmjd3 activates *Hox8–9* PGs dependent on its H3K27m3 demethylase activity, but maintains the expression of *Hox3–7* PGs independent on H3K27m3 demethylase activity. In the same way, tamoxifen rather than GSK-J4 treatment at E9.0 significantly reduced the Jmjd3 protein level on the *Hox8–13* PGs (**Supplementary Figures 5B,C**, **7C**, **13**) but only increased the H3K27me3 level on *Hox10–13* PGs instead of on *Hox8–10* PGs in E9.5 embryos (**Supplementary Figures 5B**, **6B**, **7B**, **13**). Coherently, GSK-J4 treatment at E9.0 only increased the H3K27me3 level on *Hox10–13* PGs but not on *Hox8–10* PGs (**Supplementary Figures 5A**, **6B**, **13**). These results support that Jmjd3 activates *Hox10–13* PGs dependent on H3K27m3 demethylase activity but maintains the expression of *Hox8–10* PGs independent on H3K27m3 demethylase activity at E9.5 days. Therefore, we conclude that Jmjd3 temporally activates and maintains *Hox* gene expression in mice.

Jmjd3 and Ezh2 Do Not Antagonistically Control the Axial Skeletal Patterning in Mice

Previous studies indicated that sequential activation of the *Hox* gene relies on dynamic degradation of transcription repression hallmark H3K27me3 (Soshnikova and Duboule, 2009), which

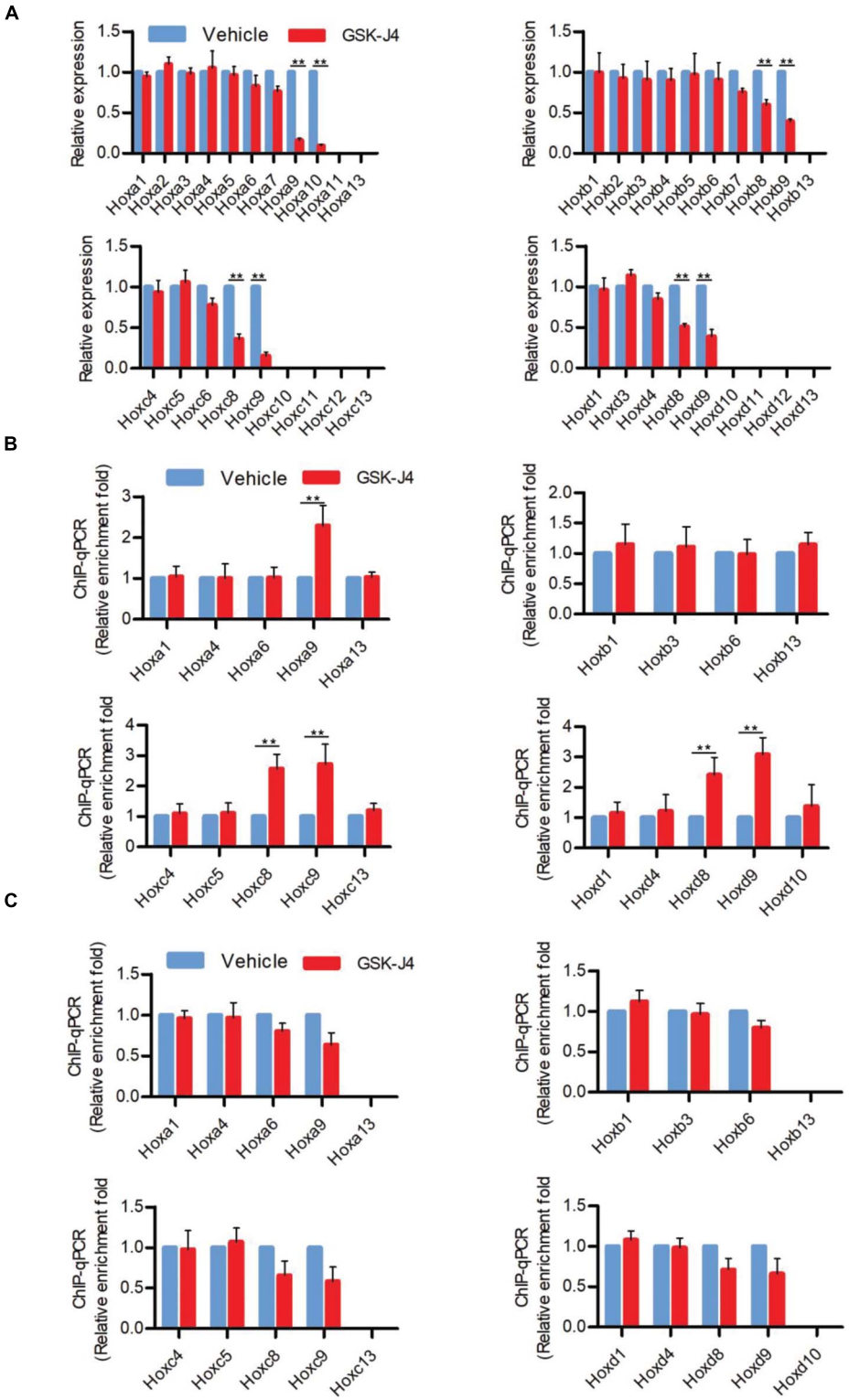

FIGURE 2 | GSK-J4 inhibits transcription of *Hox* genes by blocking the H3K27me3 demethylase activity of Jmjd3 in E8.5 mouse embryos. **(A)** The mRNA levels of *Hox* genes were determined by RT-qPCR in E8.5 embryos, which were treated by vehicle or GSK-J4 (50 mg/kg) 12 h before. **(B,C)** The ChIP-qPCR assays with antibodies specific for H3K27me3 **(B)** or Jmjd3 **(C)** on the *Hox* genes in E8.5 embryos, which were exposed to vehicle or GSK-J4 (50 mg/kg) 12 h before. Bars indicate triplicate PCR reactions ± SD. Representative results of three independent experiments are shown. $^{*}p < 0.05$, $^{**}p < 0.01$.

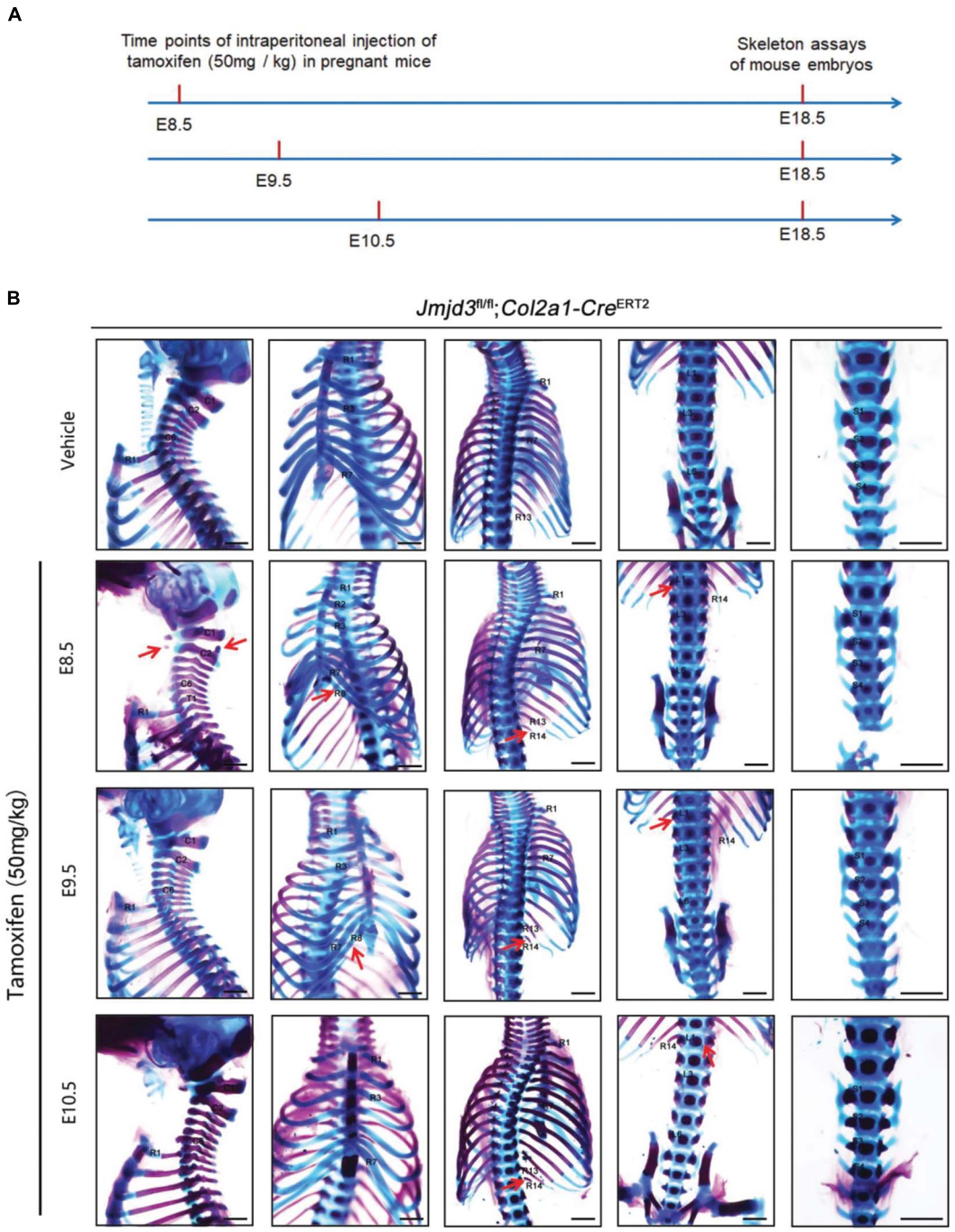

FIGURE 3 | Homeotic transformations by tamoxifen induced *Jmjd3* conditional knockout in *Col2a1* expressing chondrogenic cells at E8.5, E9.5, and E10.5 days. **(A)** Experimental design for studying the roles of Jmjd3 in chondrogenic cells on body axis patterning. **(B)** Skeletal phenotypes were prepared from E18.5 mouse embryos. The red arrow indicates homeotic transformations of axial skeletons. Frequencies of homeotic transformations are given in **Table 1**. The cervical (C), rib (R), lumbar (L), and sacral (S) vertebrae are numbered. For schematic explanation, see **Supplementary Figure 9**. Scale bar, 1 mm.

is established by histone methyltransferase Ezh2 (Cao et al., 2002; Muller et al., 2002) and erased by Kdm6 (Utx and Jmjd3) (De Santa et al., 2007; Lan et al., 2007; Lee et al., 2007). However, it is not clear whether an antagonistic interplay between Ezh2 and Jmjd3 occurs in a dynamic fashion during axial skeletal patterning. To explore this question, we crossed $Jmjd3^{fl/fl}$;$Col2a1\text{-}Cre^{ERT2}$ mice and $Ezh2^{fl/fl}$ mice to generate $Jmjd3^{fl/fl}$;$Ezh2^{fl/fl}$;$Col2a1\text{-}Cre^{ERT2}$ mice, in which both *Jmjd3* and *Ezh2* could be concurrently deleted in chondrogenic cells after tamoxifen treatment. One dose of tamoxifen treatment

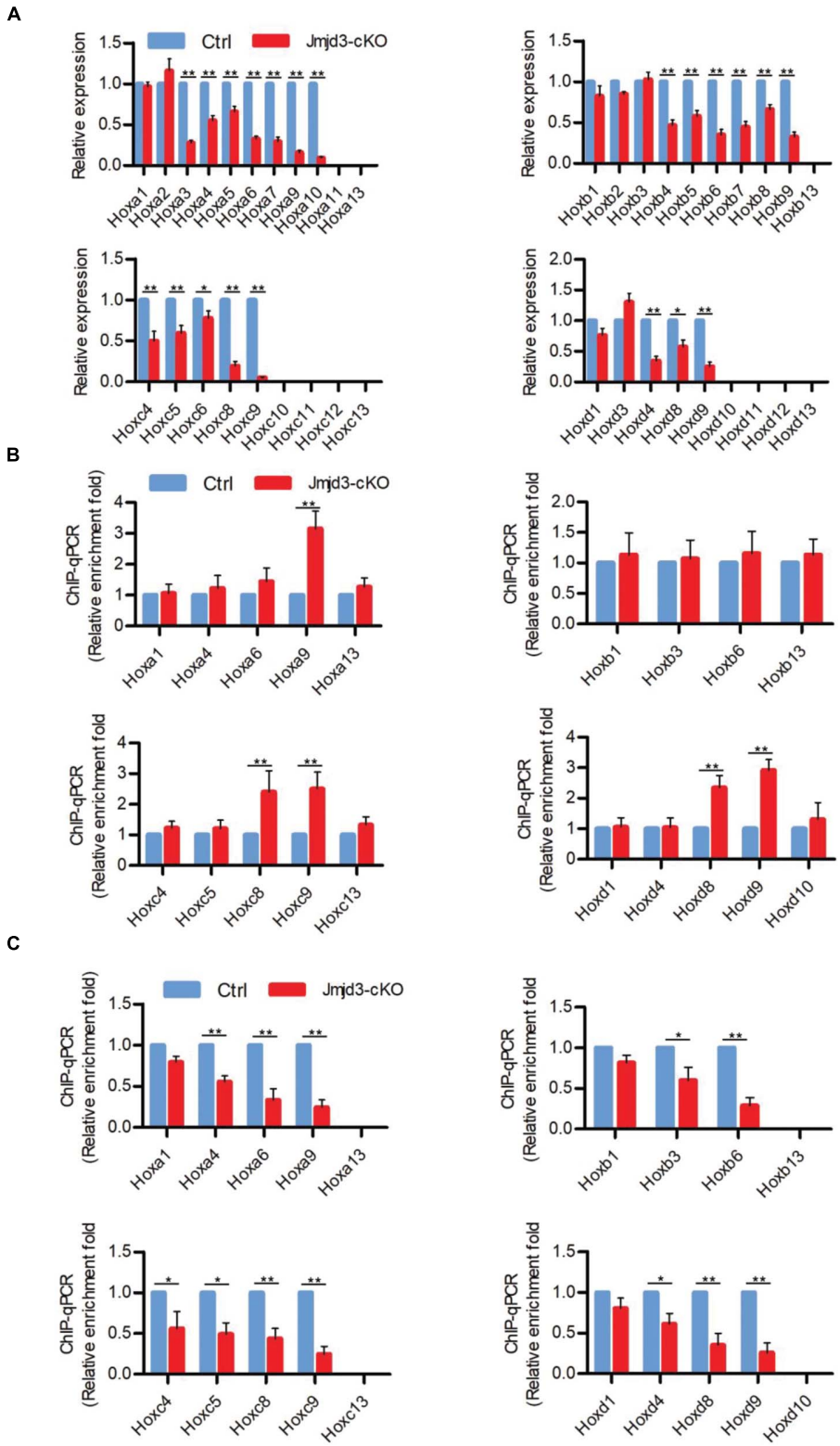

FIGURE 4 | Jmjd3 temporally activated and maintained *Hox* gene expression in mice. **(A)** The mRNA levels of *Hox* genes were determined by RT-qPCR in E8.5 control or *Jmjd3*-cKO embryos, which were treated by tamoxifen (50 mg/kg) 12 h before. **(B,C)** ChIP-qPCR assays with antibodies specific for H3K27me3 **(B)** or Jmjd3 **(C)** on the *Hox* genes in E8.5 control or *Jmjd3*-cKO embryos treated by tamoxifen (50 mg/kg) 12 h before. Bars indicate triplicate PCR reactions ± SD. Representative results of three independent experiments are shown. $^{*}p < 0.05$, $^{**}p < 0.01$.

(50 mg/kg) at E8.5 induced homeotic transformations including anterior transformation of C2 to C1 (5/12), T1 to C7 (8/12), T3 to T2 (5/12), T8 to T7 (10/12), L1 to T13 (12/12), and S1 to T6 (9/12) at the cervical, thoracic, lumbar, and sacral regions (**Supplementary Figures 8A,B**, **9A** and **Table 1**) in E18.5 *Jmjd3*$^{fl/fl}$;*Ezh2*$^{fl/fl}$;*Col2a1-Cre*^{ERT2} mouse embryos, respectively. However, these abnormalities of axial skeletal patterning were very similar to the phenotypes of *Jmjd3*-deleted mice which were treated by tamoxifen at E8.5 (**Figures 3A,B**, **Supplementary Figures 8A,B**, **9A**, and **Table 1**). Consistently, double-knockout *Jmjd3* and *Ezh2* by tamoxifen at E9.5 or E10.5 in chondrogenic cells produced similar patterning abnormalities of axial skeletons to those of *Jmjd3*-deleted mice by tamoxifen at E9.5 or E10.5, respectively (**Figures 3A,B**, **Supplementary Figures 8A,B**, **9A**, and **Table 1**). Therefore, these indicated that Jmjd3 and Ezh2 do not antagonistically and dynamically control the axial skeletal patterning of mice. Consistently, GSK-126—an inhibitor of Ezh2—treatment (100 mg/kg) at E8.5, E9.5, or E10.5 produced no broad homeotic transformations in the vertebrae along the entire body axis, except for mild increasing frequency of posterior transformation of L6 to S1 at the sacral region (**Supplementary Figure 10** and **Table 2**). Similarly, posterior transformation of L6 to S1 was the only detected homeotic transformation in *Ezh2*$^{fl/fl}$;*Prx1*-Cre (7/15) and *Ezh2*$^{fl/+}$;*Prx1*-Cre mice (10/17) (**Supplementary Figure 11** and **Table 1**). Furthermore, L6 to S1 was the only detected posterior homeotic transformation in E18.5 *Ezh2*$^{fl/fl}$;*Col2a1-Cre*^{ERT2} embryos after tamoxifen treatment at E8.5, E9.5, or E10.5, respectively (**Supplementary Figures 12A,B** and **Table 1**). Consistently, *Ezh2* deletion cannot rescue the mRNA level of *Hox6–10* PGs by *Jmjd3* knockout (**Supplementary Figures 14A,B**). Therefore, these results strongly suggested that Jmjd3 and Ezh2 do not antagonistically control the axial skeletal patterning in mice.

DISCUSSION

In this study, we demonstrated that (1) Jmjd3 regulates axial skeletal patterning and *Hox* gene temporal collinear activation with its H3K27me3 demethylase activity. (2) There is no continuously antagonistic interplay between Jmjd3 and Ezh2 in the control of body axis patterning. The results revealed that Jmjd3 rather than Ezh2 is an essential epigenetic regulator of *Hox* gene temporal collinear activation.

Jmjd3 Is an Essential Epigenetic Regulator of *Hox* Gene Temporal Collinear Activation

Hox gene temporal collinear activation is essential for the development of the body axis (Deschamps and Duboule, 2017). During the past decades, important progress has been made in the molecular regulatory mechanism of *Hox* temporal collinearity activation. For example, genetic knockout experiments confirmed that there are different *cis* regulators at the 3′ and 5′ ends to regulate the temporal collinear activation of *Hox* genes (Tschopp and Duboule, 2011). Moreover, it was found that the 3′ activated *Hox* and the 5′ silenced *Hox* were in different chromatin domains (Noordermeer et al., 2011, 2014). However, it has long been speculated that signal molecules are involved in the temporal collinear activation of *Hox* genes, such as Wnt3a (Ikeya and Takada, 2001), Fgfr1 (Partanen et al., 1998), and Gdf11 (McPherron et al., 1999). However, because these reports were not based on conditional real-time gene knockout experiments, whether these signal molecules are really required for *Hox* gene temporal collinear activation remains in need of further research. For the same reason, Naruse et al. (2017) showed that knockout of *Jmjd3* in germ cells can cause homeotic transformations in mice. However, their methods cannot prove that Jmjd3 is the regulator of *Hox* gene temporal collinear activation. In addition, it has been reported that retinoids regulate *Hox* gene temporal collinear activation *in vitro* (Chambeyron and Bickmore, 2004). However, *in vivo* experiments show that retinoids promote *Hox* gene activation at E7.5 but inhibit *Hox* gene expression at E8.5 (Kessel and Gruss, 1991). Thus, it is impossible for retinoids to regulate the whole process of *Hox* gene temporal collinear activation. In the present experiment, we demonstrated that the H3K27me3 demethylase Jmjd3 is the first identified epigenetic molecule regulating the temporal collinear activation of *Hox* genes. The evidence is as follows: among 28 histone demethylases and 17 histone methyltransferases, only Jmjd3 is successively activated and overexpressed in the development of the body axis during the period of *Hox* gene temporal activation (**Supplementary Figures 1A,B**). GSK-J4 treatment at different time points induced an alteration of the corresponding parts of the axial bone (**Figures 1A,B**, **Supplementary Figure 9A**, and **Table 1**). Finally, Jmjd3 could initiate *Hox* gene temporal collinear activation by erasing H3K27me3 (**Figures 2B**, **4B** and **Supplementary Figure 9B**).

Jmjd3 Not Only Initiates but Also Maintains the Temporal Collinear Expression of *Hox* Genes

Although Jmjd3 and Utx have proved to be H3K27m3 demethylases (Agger et al., 2007; De Santa et al., 2007; Lan et al., 2007; Lee et al., 2007), in some cases, their function did not rely on H3K27m3 demethylase activity. For example, Jmjd3 and Utx play demethylase-independent roles in chromatin remodeling in differentiated cells where the epigenetic profile is already established (Miller et al., 2010). Shpargel et al. (2014) reported that early embryonic H3K27me3 repression can be alleviated in the absence of active demethylation of Jmjd3 and Utx. Here, we found that the activation rather than maintenance of *Hox* gene expression depended on the H3K27m3 demethylase activity of Jmjd3. For instance, we found that the phenotypes induced by GSK-J4 treatment or conditional deletion of Jmjd3 by tamoxifen were very different (**Figures 1A,B**, **3A,B**, **Supplementary Figure 9A**, and **Tables 1**, **2**). At E8.5, GSK-J4 induced only anterior transformation of T8 to T7 (6/28) in the middle part of the trunk of mice (**Figures 1A,B** and **Table 2**). However, *Jmjd3* deletion at E8.5 by tamoxifen induced more extensive homeotic transformations across the whole-body axis, including C2 to C1, T1 to C7, T3 to T2, T8 to T7, L1 to T13, and S1 to T6 (**Figures 3A,B** and **Table 1**). RT-qPCR revealed

that GSK-J4 treatment at E8.0 only reduced the mRNA level on *Hox8–9* PGs (**Figure 2A** and **Supplementary Figure 5A**), while *Jmjd3* deletion by tamoxifen at E8.0 decreased the mRNA level of *Hox3–10* PGs in E8.5 mouse embryos (**Figure 4A** and **Supplementary Figure 5B**). Increasing the level of H3K27me3 on *Hox8–9* PGs in mouse embryos by both GSK-J4 treatment and *Jmjd3* deletion indicated that the removal of H3K27me3 on *Hox8–9* PGs depends on the Jmjd3 demethylase activity at the time point of E8.5 (**Figures 2B**, **4B** and **Supplementary Figures 5A,B**). However, the *Jmjd3* deletion instead of GSK-J4 treatment can reduce the mRNA level of *Hox 3–5* PGs, on which no alteration of the H3K27me3 level was detected at this time point (**Figures 2A,B**, **4A,B** and **Supplementary Figures 5A,B**), indicating that the maintaining expression of these *Hox* genes did not require the H3K27me3 demethylase of Jmjd3. In the same way, at E9.5, GSK-J4 only decreased the mRNA level of *Hox11–13* PGs and the corresponding caudal homeotic transformations (**Figures 1A,B**, **2A** and **Supplementary Figure 5A**). However, *Jmjd3* knockout can reduce the mRNA level of not only *Hox11–13* PGs but also *Hox8–10* PGs (**Figure 4A** and **Supplementary Figure 5B**), thus inducing homeotic transformations of the thoracic, lumbar, and sacral regions (**Figures 3A,B** and **Table 2**). Accordingly, these results showed that the removal of H3K27me3 on *Hox11–13* PGs instead of on *Hox8–10* PGs depends on the H3K27me3 demethylase activity of Jmjd3 (**Figures 2B**, **4B** and **Supplementary Figure 5B**). Therefore, the maintaining expression of *Hox8–10* PGs requires Jmjd3 protein rather than its enzyme activity.

No Continuous Dynamic Interplay Between Jmjd3 and Ezh2 in the Control of Body Axis Patterning

PcG or TrxG group proteins played critical roles in maintaining the expression pattern of *Hox* genes (Mallo and Alonso, 2013; Geisler and Paro, 2015). Mutations in PcG genes lead to ectopic *Hox* gene expression and consequent posterior homeotic transformations, while deletions of TrxG genes result in delayed *Hox* gene expression and consequent anterior homeotic transformations in both *Drosophila* and vertebrates (Mallo and Alonso, 2013; Geisler and Paro, 2015). Therefore, *Hox* gene expression was proposed to be dynamically and antagonistically regulated by PcG and TrxG (Hanson et al., 1999; Klymenko and Muller, 2004; Sheikh et al., 2015). Here, we detected that the homolog of TrxG group Jmjd3 loss results in anterior transformation along the axial skeleton (**Figures 1A,B**, **3A,B**, **Supplementary Figure 9A**, and **Tables 1**, **2**). However, the subunit of PcG group protein Ezh2 inactivation only produced posterior transformation of L6 to S1 (**Supplementary Figures 10–12** and **Tables 1**, **2**). Furthermore, the phenotypes of double *Jmjd3* and *Ezh2* gene-deleted mice were similar to those of *Jmjd3* knockout mice (**Figures 2A,B**, **Supplementary Figures 8A,B**, **9A**, and **Table 2**). Consistently, whole-mount *in situ* hybridization of mouse embryos at E9.5 showed that Jmjd3 was expressed more obviously in the head and trunk, while Ezh2 was expressed more strongly in the tail (**Supplementary Figure 15**). Therefore, these results strongly indicated that there is no continuous dynamic interplay between Jmjd3 and Ezh2 in the control of body axis patterning.

Axial Bone Patterning May Synchronize With Chondrogenic Differentiation in Mice

Axial skeletal formation is primarily through the process of endochondral bone formation, which starts from the differentiation of condensed mesenchymal cells to cartilaginous templates (Karsenty, 2008; Long and Ornitz, 2013). *Hox* genes are well-known patterning genes that confer identity to skeletogenic condensations (Krumlauf, 1994). There are few studies with the conditional knockout mice to explore the mechanism of spatiotemporal control of *Hox* gene transcription. Here, chondrogenic cell conditional gene knockout mice were used to address the roles of Jmjd3 during the process of mouse body axial patterning. Previously, the transcription factor Sox9 of *Col2a1* was reported be observed in the mouse embryos at E8.0 (Zhao et al., 1997; Akiyama et al., 2005). Laz reporter gene of *Col2a1*-Cre mice (Ovchinnikov et al., 2000; Nakamura et al., 2006) and *in situ* hybridization with *Col2a1* probe experiments showed that *Col2a1* could be observed in mouse embryos at E8.5 (Ng et al., 1997). Consistently, the mRNA levels of *Col2a1* and *Sox9* could be detected by RT-qPCR in E8.5 embryos of mice (**Supplementary Figure 1B**). *Jmjd3* deletion in *Col2a1*-expressing chondrogenic cells by tamoxifen treatment at E8.5 could produce homeotic transformations of the whole-body axis (**Figures 3A,B** and **Table 1**). Therefore, we suggested that axial bone patterning may synchronize with chondrogenic differentiation. This idea is further supported by a previous report that the expression of retinoic acid receptor driven by the *Col2a1* promoter could induce homeotic transformations in mice (Yamaguchi et al., 1998).

In summary, we demonstrated that the temporal collinearity activation of *Hox* genes primarily relied on Jmjd3 to erasing H3K27me3 on *Hox* genes. Jmjd3 regulates not only the initiation but also the maintenance of the temporal collinear expression of *Hox* genes. No continuous dynamic interplay was detected between Jmjd3 and Ezh2 in the control of body axis patterning. Lastly, we demonstrated that chondrogenic cells were essential for axial skeletal patterning and proposed that axial bone patterning may synchronize with chondrogenic differentiation in mice.

MATERIALS AND METHODS

Materials, methods, and associated references are described in **Supplementary Materials and Methods**.

DATA AVAILABILITY STATEMENT

The authors declare that data supporting the findings of this study are available within the article and its Supplementary Material files or from the corresponding author on request. The RNA sequencing data cited in **Supplementary Figures 1**, **2** have

been deposited in the NCBI SRA database under the accession code PRJNA673586.

ETHICS STATEMENT

The animal study was reviewed and approved by Institutional Animal Care and Use Committee at the Fourth Military Medical University.

AUTHOR CONTRIBUTIONS

FZ conceived the project, performed most of the experiments, analyzed the data, and wrote the manuscript. XZ, RJ, YW, and XW help to raise the mice, collected the samples, and performed the molecular biology experiments. All the authors helped to analyze the data and approved the final manuscript.

FUNDING

This work was supported by the National Natural Science Foundation of China (81572631 and 31000559 to FZ, 81772865 to SG, 31370981 to DZo), Shaanxi Society Development Sci-Tech Research Project (2016SF-064 to FZ, 2016SF-028 to DZn), State Key Laboratory of Cancer Biology, Fourth Military Medical University (CBSKL2019ZZ28 to FZ), and Key Research Projects of Shaanxi Province (2019ZDLSF02-01 to DZo).

SUPPLEMENTARY MATERIAL

The Supplementary Material for this article can be found online at: https://www.frontiersin.org/articles/10.3389/fcell.2021.642931/full#supplementary-material

REFERENCES

Agger, K., Cloos, P. A., Christensen, J., Pasini, D., Rose, S., Rappsilber, J., et al. (2007). UTX and JMJD3 are histone H3K27 demethylases involved in HOX gene regulation and development. *Nature* 449, 731–734. doi: 10.1038/nature06145

Akiyama, H., Kim, J. E., Nakashima, K., Balmes, G., Iwai, N., Deng, J. M., et al. (2005). Osteo-chondroprogenitor cells are derived from Sox9 expressing precursors. *Proc. Natl. Acad. Sci. U.S.A.* 102, 14665–14670. doi: 10.1073/pnas.0504750102

Alexander, T., Nolte, C., and Krumlauf, R. (2009). Hox genes and segmentation of the hindbrain and axial skeleton. *Annu. Rev. Cell Dev. Biol.* 25, 431–456. doi: 10.1146/annurev.cellbio.042308.113423

Cao, R., Tsukada, Y., and Zhang, Y. (2005). Role of Bmi-1 and Ring1A in H2A ubiquitylation and Hox gene silencing. *Mol. Cell* 20, 845–854. doi: 10.1016/j.molcel.2005.12.002

Cao, R., Wang, L., Wang, H., Xia, L., Erdjument-Bromage, H., Tempst, P., et al. (2002). Role of histone H3 lysine 27 methylation in Polycomb-group silencing. *Science* 298, 1039–1043. doi: 10.1126/science.1076997

Casaca, A., Santos, A. C., and Mallo, M. (2014). Controlling Hox gene expression and activity to build the vertebrate axial skeleton. *Dev .Dyn.* 243, 24–36. doi: 10.1002/dvdy.24007

Chambeyron, S., and Bickmore, W. A. (2004). Chromatin decondensation and nuclear reorganization of the HoxB locus upon induction of transcription. *Genes. Dev.* 18, 1119–1130. doi: 10.1101/gad.292104

Copur, O., and Muller, J. (2013). The histone H3-K27 demethylase Utx regulates HOX gene expression in *Drosophila* in a temporally restricted manner. *Development* 140, 3478–3485. doi: 10.1242/dev.097204

Copur, O., and Muller, J. (2018). Histone demethylase activity of Utx Is essential for viability and regulation of HOX Gene expression in *Drosophila*. *Genetics* 208, 633–637. doi: 10.1534/genetics.117.300421

Czermin, B., Melfi, R., McCabe, D., Seitz, V., Imhof, A., and Pirrotta, V. (2002). *Drosophila* enhancer of Zeste/ESC complexes have a histone H3 methyltransferase activity that marks chromosomal Polycomb sites. *Cell* 111, 185–196. doi: 10.1016/s0092-8674(02)00975-3

De Santa, F., Totaro, M. G., Prosperini, E., Notarbartolo, S., Testa, G., and Natoli, G. (2007). The histone H3 lysine-27 demethylase Jmjd3 links inflammation to inhibition of polycomb-mediated gene silencing. *Cell* 130, 1083–1094. doi: 10.1016/j.cell.2007.08.019

Deschamps, J., and Duboule, D. (2017). Embryonic timing, axial stem cells, chromatin dynamics, and the Hox clock. *Genes. Dev.* 31, 1406–1416. doi: 10.1101/gad.303123.117

Deschamps, J., van den Akker, E., Forlani, S., De Graaff, W., Oosterveen, T., Roelen, B., et al. (1999). Initiation, establishment and maintenance of Hox gene expression patterns in the mouse. *Int. J. Dev. Biol.* 43, 635–650.

Deschamps, J., and van Nes, J. (2005). Developmental regulation of the Hox genes during axial morphogenesis in the mouse. *Development* 132, 2931–2942. doi: 10.1242/dev.01897

Deschamps, J., and Wijgerde, M. (1993). Two phases in the establishment of HOX expression domains. *Dev. Biol.* 156, 473–480. doi: 10.1006/dbio.1993.1093

Dhar, S. S., Lee, S. H., Chen, K., Zhu, G., Oh, W., Allton, K., et al. (2016). An essential role for UTX in resolution and activation of bivalent promoters. *Nucleic Acids Res.* 44, 3659–3674. doi: 10.1093/nar/gkv1516

Favier, B., and Dolle, P. (1997). Developmental functions of mammalian Hox genes. *Mol. Hum. Reprod.* 3, 115–131. doi: 10.1093/molehr/3.2.115

Forlani, S., Lawson, K. A., and Deschamps, J. (2003). Acquisition of Hox codes during gastrulation and axial elongation in the mouse embryo. *Development* 130, 3807–3819. doi: 10.1242/dev.00573

Geisler, S. J., and Paro, R. (2015). Trithorax and Polycomb group-dependent regulation: a tale of opposing activities. *Development* 142, 2876–2887. doi: 10.1242/dev.120030

Hanson, R. D., Hess, J. L., Yu, B. D., Ernst, P., van Lohuizen, M., Berns, A., et al. (1999). Mammalian Trithorax and polycomb-group homologues are antagonistic regulators of homeotic development. *Proc. Natl. Acad. Sci. U.S.A.* 96, 14372–14377. doi: 10.1073/pnas.96.25.14372

Hashizume, R., Andor, N., Ihara, Y., Lerner, R., Gan, H., Chen, X., et al. (2014). Pharmacologic inhibition of histone demethylation as a therapy for pediatric brainstem glioma. *Nat. Med.* 20, 1394–1396. doi: 10.1038/nm.3716

Hong, S., Cho, Y. W., Yu, L. R., Yu, H., Veenstra, T. D., and Ge, K. (2007). Identification of JmjC domain-containing UTX and JMJD3 as histone H3 lysine 27 demethylases. *Proc. Natl. Acad. Sci. U.S. A.* 104, 18439–18444. doi: 10.1073/pnas.0707292104

Ikeya, M., and Takada, S. (2001). Wnt-3a is required for somite specification along the anteroposterior axis of the mouse embryo and for regulation of cdx-1 expression. *Mech. Dev.* 103, 27–33. doi: 10.1016/s0925-4773(01)00338-0

Juan, A. H., and Ruddle, F. H. (2003). Enhancer timing of Hox gene expression: deletion of the endogenous Hoxc8 early enhancer. *Development* 130, 4823–4834. doi: 10.1242/dev.00672

Karsenty, G. (2008). Transcriptional control of skeletogenesis. *Annu. Rev. Genomics Hum. Genet.* 9, 183–196. doi: 10.1146/annurev.genom.9.081307.164437

Kennison, J. A., and Tamkun, J. W. (1988). Dosage-dependent modifiers of polycomb and antennapedia mutations in *Drosophila*. *Proc. Natl. Acad. Sci. U.S.A.* 85, 8136–8140. doi: 10.1073/pnas.85.21.8136

Kessel, M., and Gruss, P. (1991). Homeotic transformations of murine vertebrae and concomitant alteration of Hox codes induced by retinoic acid. *Cell* 67, 89–104. doi: 10.1016/0092-8674(91)90574-i

Klymenko, T., and Muller, J. (2004). The histone methyltransferases Trithorax and Ash1 prevent transcriptional silencing by Polycomb group proteins. *EMBO Rep.* 5, 373–377. doi: 10.1038/sj.embor.7400111

Kmita, M., and Duboule, D. (2003). Organizing axes in time and space; 25 years of colinear tinkering. *Science* 301, 331–333. doi: 10.1126/science.1085753

Kondrashov, N., Pusic, A., Stumpf, C. R., Shimizu, K., Hsieh, A. C., Ishijima, J., et al. (2011). Ribosome-mediated specificity in Hox mRNA translation and vertebrate tissue patterning. *Cell* 145, 383–397. doi: 10.1016/j.cell.2011.03.028

Krumlauf, R. (1994). Hox genes in vertebrate development. *Cell* 78, 191–201. doi: 10.1016/0092-8674(94)90290-9

Krumlauf, R. (2018). Hox genes, clusters and collinearity. *Int. J. Dev. Biol.* 62, 659–663. doi: 10.1387/ijdb.180330rr

Kuzmichev, A., Nishioka, K., Erdjument-Bromage, H., Tempst, P., and Reinberg, D. (2002). Histone methyltransferase activity associated with a human multiprotein complex containing the Enhancer of Zeste protein. *Genes. Dev.* 16, 2893–2905. doi: 10.1101/gad.1035902

Lan, F., Bayliss, P. E., Rinn, J. L., Whetstine, J. R., Wang, J. K., Chen, S., et al. (2007). A histone H3 lysine 27 demethylase regulates animal posterior development. *Nature* 449, 689–694. doi: 10.1038/nature06192

Lee, M. G., Villa, R., Trojer, P., Norman, J., Yan, K. P., Reinberg, D., et al. (2007). Demethylation of H3K27 regulates polycomb recruitment and H2A ubiquitination. *Science* 318, 447–450. doi: 10.1126/science.1149042

Lewis, E. B. (1978). A gene complex controlling segmentation in *Drosophila*. *Nature* 276, 565–570. doi: 10.1038/276565a0

Li, L., Liu, B., Wapinski, O. L., Tsai, M. C., Qu, K., Zhang, J., et al. (2013). Targeted disruption of Hotair leads to homeotic transformation and gene derepression. *Cell Rep.* 5, 3–12. doi: 10.1016/j.celrep.2013.09.003

Liu, P., Wakamiya, M., Shea, M. J., Albrecht, U., Behringer, R. R., and Bradley, A. (1999). Requirement for Wnt3 in vertebrate axis formation. *Nat. Genet.* 22, 361–365. doi: 10.1038/11932

Logan, M., Martin, J. F., Nagy, A., Lobe, C., Olson, E. N., and Tabin, C. J. (2002). Expression of Cre Recombinase in the developing mouse limb bud driven by a Prxl enhancer. *Genesis* 33, 77–80. doi: 10.1002/gene.10092

Long, F., and Ornitz, D. M. (2013). Development of the endochondral skeleton. *Cold Spring Harb. Perspect. Biol.* 5:a008334. doi: 10.1101/cshperspect.a008334

Mallo, M., and Alonso, C. R. (2013). The regulation of Hox gene expression during animal development. *Development* 140, 3951–3963. doi: 10.1242/dev.068346

McCabe, M. T., Ott, H. M., Ganji, G., Korenchuk, S., Thompson, C., Van Aller, G. S., et al. (2012). EZH2 inhibition as a therapeutic strategy for lymphoma with EZH2-activating mutations. *Nature* 492, 108–112. doi: 10.1038/nature11606

McPherron, A. C., Lawler, A. M., and Lee, S. J. (1999). Regulation of anterior/posterior patterning of the axial skeleton by growth/differentiation factor 11. *Nat. Genet.* 22, 260–264. doi: 10.1038/10320

Miller, S. A., Mohn, S. E., and Weinmann, A. S. (2010). Jmjd3 and UTX play a demethylase-independent role in chromatin remodeling to regulate T-box family member-dependent gene expression. *Mol. Cell* 40, 594–605. doi: 10.1016/j.molcel.2010.10.028

Mongera, A., Michaut, A., Guillot, C., Xiong, F., and Pourquie, O. (2019). Mechanics of anteroposterior axis formation in vertebrates. *Annu. Rev. Cell Dev. Biol.* 35, 259–283. doi: 10.1146/annurev-cellbio-100818-125436

Montavon, T., and Soshnikova, N. (2014). Hox gene regulation and timing in embryogenesis. *Semin. Cell Dev. Biol.* 34, 76–84. doi: 10.1016/j.semcdb.2014.06.005

Muller, J., Hart, C. M., Francis, N. J., Vargas, M. L., Sengupta, A., Wild, B., et al. (2002). Histone methyltransferase activity of a *Drosophila* Polycomb group repressor complex. *Cell* 111, 197–208. doi: 10.1016/s0092-8674(02)00976-5

Nakamura, E., Nguyen, M. T., and Mackem, S. (2006). Kinetics of tamoxifen-regulated Cre activity in mice using a cartilage-specific CreER(T) to assay temporal activity windows along the proximodistal limb skeleton. *Dev. Dyn.* 235, 2603–2612. doi: 10.1002/dvdy.20892

Naruse, C., Shibata, S., Tamura, M., Kawaguchi, T., Abe, K., Sugihara, K., et al. (2017). New insights into the role of Jmjd3 and Utx in axial skeletal formation in mice. *FASEB J.* 31, 2252–2266. doi: 10.1096/fj.201600642r

Neijts, R., Amin, S., van Rooijen, C., Tan, S., Creyghton, M. P., de Laat, W., et al. (2016). Polarized regulatory landscape and Wnt responsiveness underlie Hox activation in embryos. *Genes. Dev.* 30, 1937–1942. doi: 10.1101/gad.285767.116

Ng, L. J., Wheatley, S., Muscat, G. E., Conway-Campbell, J., Bowles, J., Wright, E., et al. (1997). SOX9 binds DNA, activates transcription, and coexpresses with type II collagen during chondrogenesis in the mouse. *Dev. Biol.* 183, 108–121. doi: 10.1006/dbio.1996.8487

Noordermeer, D., Leleu, M., Schorderet, P., Joye, E., Chabaud, F., and Duboule, D. (2014). Temporal dynamics and developmental memory of 3D chromatin architecture at Hox gene loci. *Elife* 3:e02557.

Noordermeer, D., Leleu, M., Splinter, E., Rougemont, J., De Laat, W., and Duboule, D. (2011). The dynamic architecture of Hox gene clusters. *Science* 334, 222–225. doi: 10.1126/science.1207194

Ntziachristos, P., Tsirigos, A., Welstead, G. G., Trimarchi, T., Bakogianni, S., Xu, L., et al. (2014). Contrasting roles of histone 3 lysine 27 demethylases in acute lymphoblastic leukaemia. *Nature* 514, 513–517. doi: 10.1038/nature13605

Ovchinnikov, D. A., Deng, J. M., Ogunrinu, G., and Behringer, R. R. (2000). Col2a1-directed expression of Cre recombinase in differentiating chondrocytes in transgenic mice. *Genesis* 26, 145–146. doi: 10.1002/(sici)1526-968x(200002)26:2<145::aid-gene14>3.0.co;2-c

Partanen, J., Schwartz, L., and Rossant, J. (1998). Opposite phenotypes of hypomorphic and Y766 phosphorylation site mutations reveal a function for Fgfr1 in anteroposterior patterning of mouse embryos. *Genes. Dev.* 12, 2332–2344. doi: 10.1101/gad.12.15.2332

Piunti, A., and Shilatifard, A. (2016). Epigenetic balance of gene expression by Polycomb and COMPASS families. *Science* 352:aad9780. doi: 10.1126/science.aad9780

Sheikh, B. N., Downer, N. L., Phipson, B., Vanyai, H. K., Kueh, A. J., McCarthy, D. J., et al. (2015). MOZ and BMI1 play opposing roles during Hox gene activation in ES cells and in body segment identity specification in vivo. *Proc. Natl. Acad. Sci. U.S.A.* 112, 5437–5442. doi: 10.1073/pnas.1422872112

Shen, X., Liu, Y., Hsu, Y. J., Fujiwara, Y., Kim, J., Mao, X., et al. (2008). EZH1 mediates methylation on histone H3 lysine 27 and complements EZH2 in maintaining stem cell identity and executing pluripotency. *Mol. Cell* 32, 491–502. doi: 10.1016/j.molcel.2008.10.016

Shpargel, K. B., Starmer, J., Yee, D., Pohlers, M., and Magnuson, T. (2014). KDM6 demethylase independent loss of histone H3 lysine 27 trimethylation during early embryonic development. *PLoS Genet.* 10:e1004507. doi: 10.1371/journal.pgen.1004507

Simon, J., Chiang, A., and Bender, W. (1992). Ten different Polycomb group genes are required for spatial control of the abdA and AbdB homeotic products. *Development* 114, 493–505. doi: 10.1242/dev.114.2.493

Soshnikova, N., and Duboule, D. (2009). Epigenetic temporal control of mouse Hox genes in vivo. *Science* 324, 1320–1323. doi: 10.1126/science.1171468

Srivastava, S., Dhawan, J., and Mishra, R. K. (2015). Epigenetic mechanisms and boundaries in the regulation of mammalian Hox clusters. *Mech. Dev.* 138(Pt 2), 160–169. doi: 10.1016/j.mod.2015.07.015

Tschopp, P., and Duboule, D. (2011). A genetic approach to the transcriptional regulation of Hox gene clusters. *Annu. Rev. Genet.* 45, 145–166. doi: 10.1146/annurev-genet-102209-163429

Wellik, D. M. (2009). Hox genes and vertebrate axial pattern. *Curr. Top. Dev. Biol.* 88, 257–278. doi: 10.1016/s0070-2153(09)88009-5

Yamaguchi, M., Nakamoto, M., Honda, H., Nakagawa, T., Fujita, H., Nakamura, T., et al. (1998). Retardation of skeletal development and cervical abnormalities in transgenic mice expressing a dominant-negative retinoic acid receptor in chondrogenic cells. *Proc. Natl. Acad. Sci. U.S.A.* 95, 7491–7496. doi: 10.1073/pnas.95.13.7491

Ye, L., Fan, Z., Yu, B., Chang, J., Al Hezaimi, K., Zhou, X., et al. (2012). Histone demethylases KDM4B and KDM6B promotes osteogenic differentiation of human MSCs. *Cell Stem Cell* 11, 50–61. doi: 10.1016/j.stem.2012.04.009

Young, T., Rowland, J. E., van de Ven, C., Bialecka, M., Novoa, A., Carapuco, M., et al. (2009). Cdx and Hox genes differentially regulate posterior axial growth in mammalian embryos. *Dev. Cell* 17, 516–526. doi: 10.1016/j.devcel.2009.08.010

Zhang, F., Xu, L., Xu, L., Xu, Q., Li, D., Yang, Y., et al. (2015). JMJD3 promotes chondrocyte proliferation and hypertrophy during endochondral bone formation in mice. *J. Mol. Cell Biol.* 7, 23–34. doi: 10.1093/jmcb/mjv003

Zhao, Q., Eberspaecher, H., Lefebvre, V., and De Crombrugghe, B. (1997). Parallel expression of Sox9 and Col2a1 in cells undergoing chondrogenesis. *Dev. Dyn.* 209, 377–386. doi: 10.1002/(sici)1097-0177(199708)209:4<377::aid-aja5>3.0.co;2-f

Zheng, L., Xu, L., Xu, Q., Yu, L., Zhao, D., Chen, P., et al. (2018). Utx loss causes myeloid transformation. *Leukemia* 32, 1458–1465. doi: 10.1038/s41375-018-0011-6

Conflict of Interest: The authors declare that the research was conducted in the absence of any commercial or financial relationships that could be construed as a potential conflict of interest.